

EMD-BASED ANALYSIS OF RAT EEG DATA FOR SLEEP STATE CLASSIFICATION

Süleyman Baykut^{1,2}, Paulo Gonçalves², Pierre-Hervé Luppi³, Patrice Abry⁴
Edmundo Pereira de Souza Neto^{4,5} and Damien Gervasoni³

¹*Department of Electronics and Communications Engineering, Istanbul Technical University, Istanbul, Turkey*

²*INRIA-RESO, LIP, Ecole Normale Supérieure de Lyon, Lyon, France*

³*Physiopathologie des Réseaux Neuronaux du Cycle Veille-Sommeil, UMR5167 CNRS, Université Claude Bernard, Lyon, France*

⁴*Laboratoire de Physique, UMR 5672 CNRS, Ecole Normale Supérieure de Lyon, Lyon, France*

⁵*Service d'Anesthésie Réanimation, Hôpital Pierre Wertheimer, Hospices Civils de Lyon, Bron, France*

Keywords: Automatic Sleep State Classification, Empirical Mode Decomposition, Rat EEG.

Abstract: In this paper Empirical Mode Decomposition (EMD)-based features from single-channel electroencephalographic (EEG) data are proposed for rat's sleep state classification. The classification performances of the EMD-based features and some classical power spectrum density (PSD)-based features are compared. Supported by experiments on real EEG data, we demonstrate that classification performances can significantly improve, by simply substituting EMD to PSD in features extraction. This is in noticeably due to the natural adaptivity of EMD which show more robust to subjects variability.

1 INTRODUCTION

EEG signals are widely used to study the basic aspects of the brain activities in human and/or in animals. EEG data show variations related to the different brain states during sleep which make EEG an important tool in sleep studies (Robert et al., 1999; Vyazovskiy et al., 2002; Estrada et al., 2004; Hese et al., 2001; Vivaldi and Bassi, 2006; Corsi-Cabrera et al., 2001). Objective staging of the sleep states by visual analysis of EEG data is a time consuming and rather subjective process, as staging agreement between different experts is around 80 – 90% (Gervasoni et al., 2004; Robert et al., 1999). In recent years, the researches focused on defining new methods, mostly utilizing EEG data, in order to provide an automatic and more objective staging of the brain states. However, due to the complexity and to the subject variability of EEG signals, automatic sleep classification still remains a challenging issue.

Automatic sleep state classification based on EEG data has been performed by a large number of techniques relying on time, frequency or wavelet domain features, such as EEG amplitudes, zero crossing counting, harmonic analysis, Hjorth parameters, specific bandwidths' energies (δ, θ, σ), bispectra (Ning

et al., 1990), to cite but a few.

In most studies dealing with automatic quantitative classification of sleep states, frequency domain features seem to be preferred. In particular, Power Spectrum Density (PSD)-based classifications rely on the energy carried out in different frequency intervals, even if a unanimous consensus about the definition of sensitive bandwidths is still missing (Robert et al., 1999; Corsi-Cabrera et al., 2001). It is also noticed that most representative EEG activities may vary between sleep states and between different subjects (Corsi-Cabrera et al., 2001). Moreover, to be fully relevant, PSD-based methods require the data to be stationary over the analyzed epoch. This is another severe limitation when dealing with EEG signals which by nature are non-stationary as it is the case for most biomedical signals. For all these reasons, a method that is adaptive (data-driven), less sensitive to subject heterogeneity and robust to non-stationary data is certainly worth investigating.

Empirical Mode Decomposition (EMD) is known to be a fully data-driven technique which automatically extracts meaningful oscillating components (intrinsic modes) that underlie the signal (Huang et al., 1998; Rilling et al., 2003). Furthermore, as it acts locally in time, EMD does not require the analyzed

signal to be stationary. The main goal of this study is then to underline how the inherent advantages of EMD can sensibly strengthen the features' extraction and improve the sleep state classification.

The article is organized as follows. Data and methods are described in Sections 2 and 3, respectively. Section 4 presents and compares the classification performances of both PSD and EMD-based approaches. We conclude and discuss possible extensions of this work in Section 5.

2 MATERIALS

In order to reduce the number of experimented animals, we advisedly re-used for this study a data set originally obtained from previous experiments. In these experiments, adult male Sprague Dawley rats (250-300 g) were chronically implanted for polygraphic recordings under general anesthesia (Ketamine / Xylazine, 90 mg/kg and 5mg/kg respectively). Briefly, three stainless steel EEG screws were inserted into the skull over the frontal, parietal and occipital cortices, with a reference electrode placed over the cerebellum. Two stainless wires were inserted into the neck muscles. All electrodes were linked to a connector cemented to the skull with dental acrylic. Post-operative analgesia was ensured by oral administration of carprofen (Rimadyl[®], 0.5 mg / 100 g / 24 h). After ten days of recovery from the surgical procedure, the rats were individually habituated to the recording chamber and cable under a 12 hour light/dark cycle (lights on at 7:00 A.M.) with water and food ad libitum. All procedures were in accordance with the National Institute of Health guidelines for animal care and were approved by our local institutional ethics committee for animal experimentation. From each rat, three referential EEG and one bipolar EMG signals were amplified and filtered (bandwidth 1-250 Hz) using a preamplifier headstage and a multichannel amplifier (MCP Plus, Alpha-Omega Engineering, Nazareth, Israel), and sampled at 512 Hz using an analog to digital converter (Cambridge Electronic Design, Cambridge, UK). In this study, the data set from 6 rats are analyzed. Data files were manually scored by 10-seconds epochs using EEG and EMD magnitude criteria defined in the four distinct papers (Gervasoni et al., 2004), (Gottesmann et al., 1976), (Timo-Iaria et al., 1970), (Winson, 1974). Although the epochs were scored by two scorers with an inter-rater agreement of 85%, here the result from only one scorer was used. Blind repeated scoring was not performed in this study. Three sleep states are identified;

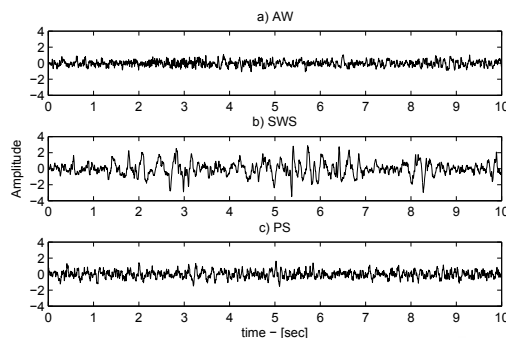


Figure 1: Rat EEG Signals at a) Awake, b) Slow Wave Sleep, c) Paradoxical Sleep.

1. Awake (AW): AW epochs are characterized by low amplitude EEGs with high θ (5-9 Hz) and γ (30-55 Hz) power density and a high amplitude EMG with phasic bursts.
2. Slow Wave Sleep (SWS): SWS epochs are identified by high amplitude EEG with a high δ (1-4 Hz) and spindles (10-14 Hz) power density and a low amplitude EMG.
3. Paradoxical Sleep (PS): PS (Rapid Eye Movement) was identified by a low amplitude EEG with a predominant θ rhythm (5-9 Hz) and a concomitant low amplitude EMG reflecting the typical muscular atonia.

In Figure 1 a-c, examples of 10-seconds rat EEG signals from frontal cortex derivation are plotted for AW, SWS and PS states, respectively.

All the segments with saturated sample points are discarded from the analysis. In the data set, only the three main sleep states are identified. However, it is known that, at the sleep cycles, middle transition states are also present between main sleep states (Gervasoni et al., 2004). These transition states may create ambiguity during the search for best representative and discriminative features. Therefore, the transition segments that may correspond to possible transition states are also excluded from the data base. The numbers of remaining segments after data cleaning are described in Table 1 for all states and from each of the six rats.

Table 1: The number of segments at each sleep states for six rats.

Rat	Time \ segments	# AW	# SWS	# PS
1	208 min \ 1253	863	198	192
2	91 min \ 547	200	135	212
3	115 min \ 689	352	188	149
4	241 min \ 1446	930	467	49
5	194 min \ 1162	766	232	164
6	310 min \ 1860	784	869	207

Table 2: Spectral Energy Bands.

Band	Bandwidth (Hz)
δ_1	0.5 - 2.5
δ_2	2.5 - 4.0
θ_1	4.0 - 6.0
θ_2	6.0 - 8.0
α	8.0 - 12.0
β_1	12.0 - 20.0
β_2	20.0 - 45.0

3 METHODS

This section starts presenting two classical approaches based on the estimated power spectrum density of EEG time series. After describing the PSD-based techniques, new feature sets based on EMD analysis are proposed. Each data segment is normalized before PSD or EMD analyses in order to have unit energy within each 10-seconds segment.

3.1 PSD-based Features

3.1.1 Relative Bandwidths' Energies

Several studies have shown relevance in parsing EEG signals into different frequency bands. For instance, (Goeller and Sinton, 1989) suggests to consider four bands 1-3 Hz, 4-6 Hz, 6-10 Hz and 11-25 Hz; according to (Ruigt et al., 1989), seven bands are relevant: 1-3 Hz, 3-6 Hz, 6-9 Hz, 9.5-20 Hz, 20-45 Hz, 49-51 Hz and 1-45 Hz; as for (Neckelmann et al., 1994), only four bands are necessary: 0.5-5 Hz, 6-9 Hz, 11-16Hz, 20-60.5 Hz. We chose in the present study to divide the frequency axis into seven different energy bands as proposed in (Estrada et al., 2004; Hese et al., 2001) and reported in Table 2.

The normalized PSD is estimated for each 10 seconds EEG segment, and then partially integrated over these seven frequency intervals. The resulting energies serve as input features of the sleep state classification.

3.1.2 PSD-based Spectral Energy Ratios

In the second PSD-based approach developed in (Gervasoni et al., 2004), two specific spectral energy ratios are defined and used as input features of a supervised classifier. In (Gervasoni et al., 2004), Local Field Potential (LFP) data is analyzed in order to examine sleep state transitions. Four frequency bands are defined: 0.5-20Hz, 0.5-55H, 0.5-4.5Hz, 0.5-9Hz and

then the spectral amplitude ratios, r_1 and r_2 , are obtained by dividing the integrated spectral amplitudes over defined frequency bands:

$$r_1 = \frac{\int_{0.5Hz}^{20Hz} P(f) df}{\int_{0.5Hz}^{55Hz} P(f) df} \quad r_2 = \frac{\int_{0.5Hz}^{4.5Hz} P(f) df}{\int_{0.5Hz}^{9Hz} P(f) df} \quad (1)$$

where $P(f)$ denotes the spectral amplitudes over the frequency f . These ratios are heuristically chosen after a thorough search in order to obtain the best separation of states. Numerators of the ratios are included in the denominators to obtain more symmetrical distributions. The feature space for classification is constructed by two variables (r_1, r_2) calculated from each segment.

3.2 EMD-based Features

EMD is an entirely data-driven (adaptive) method that iteratively decomposes the analyzed signal into a set of components called Intrinsic Mode Functions (IMF) (Huang et al., 1998). In contrast with the Fourier or the wavelet analyses, EMD adaptively extracts the intrinsic components that compose the signal without necessitating to choose any a priori fixed basis. The core of the algorithm is the so-called "sifting procedure" which, locally in time, isolates the fastest oscillation in the signal. The resulting (possibly non-stationary) component, referred to as the first intrinsic mode function (IMF), is an amplitude and frequency modulated waveform that corresponds to the signal details at the finest time scales. This IMF is subtracted from the original signal, and the same adaptive procedure is applied to the remainder (low-pass approximation) to identify the second IMF, and recursively for the next ones.

EMD has been successfully used in many biological signal processing applications (see e.g. (Ziqiang and Puthusserypady, 2007; Torres et al., 2007; Sharabaty et al., 2006)), and we believe that EMD-based features are also promising candidates for a more robust sleep state classification.

EMD is applied to each of the EEG signal examples shown in Figure 1 and the first 8 IMFs of each signal are displayed in Figure 2-a. It was observed that a N points time series generally decomposes into $\log_2(N)$ IMFs (Huang et al., 1998; Rilling et al., 2003). In our case, we most often obtained between 10 and 12 IMFs but only the first 8 are systematically considered as the frequency content of the remainders lay below the physiologically meaningful bandwidth ($< 0.5Hz$). As it can be seen in the figure, the IMFs reproduce the non-stationarities of the signal at different characteristic time scales.

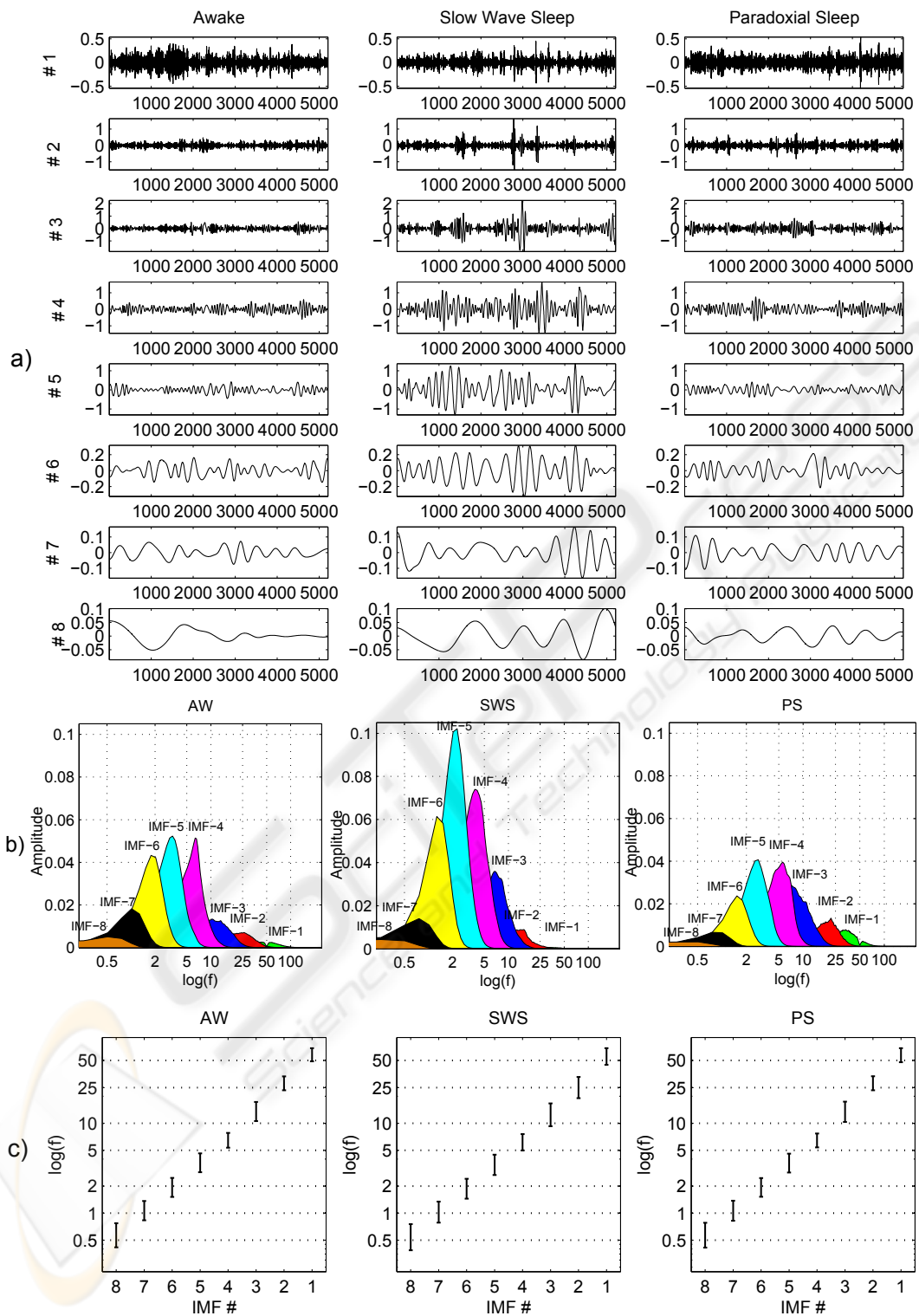


Figure 2: a) The first 8 IMFs of EEG Signals for AW (the 1st column), for SWS (the 2nd column) and for PS (the 3rd column) states; b) Average PSD of IMFs at the states AW, SWS and PS (from left to right respectively); c) The logarithm of mean values and the standard deviations of the peak frequencies of IMF spectra (EEG data segments are taken from rat-1).

Note that, for broad band signals such as EEG, EMD behaves like a dyadic filter bank (Flandrin et al., 2003). In Figure 2-b, average PSDs of IMFs obtained from EEG segments (at AW, SWS and PS states) are given. It can be observed that the frequency structures of the automatically generated IMFs are similar to that of artificially pre-defined EEG bands. For example, the frequency content of the first IMF approximately corresponds to the γ band ($>30\text{Hz}$), whereas the second IMF overlaps with the β band ($13 - 30\text{ Hz}$). The third and the fourth IMFs also coincide with the α ($8 - 13\text{ Hz}$) and θ ($3.5 - 8\text{ Hz}$) bands. A still open question though, is to determine to which extent these adaptively identified bandwidths correspond to physical phenomena. Note that the frequency regions that are automatically extracted by EMD are variable, i.e. they are changing adaptively with the analyzed signal. This can be seen from Figure 2-b that compares the IMF spectra corresponding to the different states. Moreover, the frequency peak distribution (mean and variance) of each IMF spectrum, displayed as box plots in Figure 2-c, show that characteristic modes of a given state can also vary along time.

3.2.1 EMD-based Band Energies

As it is seen in Figure 2-b, the energies at some scales are noticeably different for different states which can be convenient for classification. Therefore, energies of eight IMFs are individually considered as features for sleep staging. This approach is similar to the PSD-based relative frequency band energy features given in Section 3.1.1. However, instead of defining fixed bands beforehand, the bands are automatically selected by the method.

3.2.2 EMD-based Spectral Energy Ratios

By considering the same frequency bands defined in Section 3.1.2 the EMD-based spectral ratios can approximately mimic the PSD-based spectral ratios. It is approximately identified which IMF lie in which bandwidths considered in the energy ratios r_1 and r_2 defined in (1). The EMD based energy ratios are then constructed as below:

$$r_1 = \frac{\sum_{i \in \{2, \dots, 7\}} P_{IMF_i}}{\sum_{i \in \{1, \dots, 7\}} P_{IMF_i}} \quad r_2 = \frac{\sum_{i \in \{5, \dots, 7\}} P_{IMF_i}}{\sum_{i \in \{4, \dots, 7\}} P_{IMF_i}} \quad (2)$$

Here P_{IMF_i} is the energy of the i^{th} IMF.

3.2.3 EMD-based New Spectral Ratios

EMD provide limited number of naturally divided frequency bands which make possible to search for ad-

ditional features. In Figure 3, the energy spectra of IMFs are plotted for three sleep states. All six rats' data are combined and the mean and the standard deviations of the IMF energies are calculated. This figure is utilized to search for new energy ratios that may provide better separation of the classes.

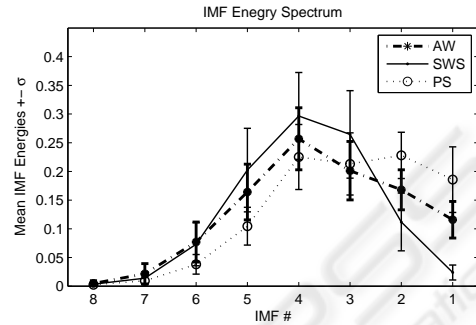


Figure 3: IMF Energy Spectra (the mean and the standard deviation of the IMF energies) of three sleep states.

We define two new ratios. The first ratio is defined for separation of AW and SWS states. It is slightly different than the ratio in (2) (6^{th} and the 7^{th} IMF energies are removed from the ratio since they are not significantly different for AW and SWS states as it is seen in Figure 3).

The second ratio is defined for the separation of AW and PS states. It is observed in Figure 3 that the energies at the first two IMFs obtained from PS state are higher than the energies of IMFs obtained from AW state. In contrast, the energies of IMFs from AW at last four scales (5, 6, 7, 8) are higher than the energies of IMFs from PS state. Considering these observations, the second ratio is defined as the total energy of the first two IMFs over the total energy of the last four IMFs. Similar to the previously defined ratios, the denominator includes also the numerator components:

$$r_1 = \frac{\sum_{i \in \{2, \dots, 5\}} P_{IMF_i}}{\sum_{i \in \{1, \dots, 5\}} P_{IMF_i}} \quad r_2 = \frac{\sum_{i \in \{1, 2\}} P_{IMF_i}}{\sum_{i \in \{1, 2, 5, 6, 7, 8\}} P_{IMF_i}} \quad (3)$$

The two PSD-based and the three EMD-based feature sets defined in the previous Sections are used as input features of a supervised classifier of EEG data. Results are compared in the next section.

4 STATISTICAL ANALYSIS AND RESULTS

A simple supervised classifier is used by fitting a multivariate normal density to each class. Several classi-

fication parameters are provided for each feature set as a measure of classification performances:

- Sensitivity (Sns.) and Specificity (Sp.): Sensitivity is the proportion of the correctly identified (true positives) segments that actually belong to the class and specificity is the proportion of the correctly identified (true negatives) segments that actually do not belong to the class.
- Omission Error (ϵ_o) and Commission Error (ϵ_c): ϵ_o is the proportion of the omitted segments that actually belong to the class ($\epsilon_o = 1 - \text{Sns.}$). ϵ_c is the proportion of the segments classified as the corresponding class where they actually do not belong to the class ($\epsilon_c = 1 - \text{Sp.}$).
- Overall Accuracy (Acc.): Accuracy is the proportion of the truly classified segments in the whole population.
- Kohen's Kappa (κ): κ is a measure of agreement between the manual and automatic staging. $1 > \kappa > 0.81$ indicates almost perfect agreement, whereas $0.8 > \kappa > 0.61$ and $0.6 > \kappa > 0.41$ indicate substantial and moderate agreements respectively. This parameter is different from the overall agreement in the sense that it removes the effects of the agreements occurred by chance. κ is calculated as: $\kappa = \frac{P_0 - P_c}{1 - P_c}$ where P_0 is the overall agreement between manual and automatic staging, and P_c is the expected agreement by chance (Cohen, 1960).
- Concordance Table (Confusion Matrix): The fraction of the data which was classified as each of the existing classes are given in concordance tables. In these tables, each row represents the actual class whereas each column represents the predicted class.

We hold two different scenarios of classification experiment.

- Self Classification: In the first group experiment, all the data from the six rats are gathered and a 5-folds cross validation is used. Since the training and the test data are selected from the same data pool, this experiment is called self-classification throughout the paper.
- Cross Classification: In the second group experiment, we train the classifier with mixed data coming from only five rats, and test the algorithm with the remaining sixth rat's EEG. This procedure is repeated for all possible combinations of the rats and only the mean classification rates are provided. We refer to this experiment as cross-classification. The aim of this experiment

is to assess the robustness of the features to inter-individual variability.

4.1 Self-classification Experiments

4.1.1 PSD-based Band Energies vs. EMD-based Band Energies

Self-classification results (mean \pm standard deviation of each performance parameters) obtained by the PSD-based and EMD-based band energy features are given in Tables 3 and 4. It is observed in the concordance tables that the separation of SWS class from the other two classes is attains a high matching score (with $\sim 96 - 98\%$) by both PSD and EMD based features. On the other hand, separation of AW and PS states is more arduous. Yet, the energies computed over the adaptively EMD-selected bandwidths provide relatively better results. Indeed, the omission error of AW state decreases of about 7% and the commission error of PS state gains 18%. As we can see, simply replacing the pre-fixed bands with the ones that are automatically identified by EMD provides a 3% increase on the overall accuracy and a 0.04 melioration of κ index. This shows that even within the same rat's EEG, the frequency content relative to a given state, can vary from one time segment to the other (as it can be seen in Figure 2-c), and that automatic band selection is an encouraging alternative to handle this non-stationarity.

4.1.2 PSD-based Energy Ratios vs. EMD-based Energy Ratios

Self classification results for PSD-based spectral ratios and for their EMD-based counterpart are given in Table 5 and 6, respectively. Similarly to the band energy features, SWS class is easily distinguished from the other two classes ($\sim 96 - 97\%$ agreement) by both PSD and EMD-based ratios. However, discrimination of AW and PS classes is relatively worse. For PSD-based ratios, 23% of AW segments are classified as PS and 15% of PS segments are classified as AW. By using EMD-based ratios, these percentages lower to 18% and 12% respectively. Overall accuracy also gets better, with a 3% upgrade, whereas κ index increases of about +0.04.

As it is explained in Section 3.2.3, in order to have better separation between AW and PS classes, new EMD-based ratios were defined. The classification results are provided in Table 7. Compared to the PSD-based ratios' results of Table 5, EMD-based new ratios pull the omission for AW class from 24% down to 17%. Omission of PS class also decreases from 16% to 11%. Overall accuracy improves by 4.6% and the

κ gain is 0.07. For similar reasons to the ones evoked in the preceding paragraph, it is very likely that the adaptivity of EMD turns the energy ratios more robust to non-stationarities.

4.2 Cross-classification Experiments

The aim of this experiment is to investigate the robustness of the feature sets to the inter-individual variability. The results obtained for the cross classification experiment are presented in Table 8. As for the self classification, EMD features globally provide better classification performances. Again the differences stem from a better separation between AW and PS states. For example, compared to PSD-based energy ratios, EMD-based new energy ratios increases the sensitivity for AW and PS classes by 9% and 7%, respectively. The specificities also improve (4% and 13%), as well as the overall accuracy (about 5.5%) and the κ index which raises by +0.09. Improvements of the same order of magnitude can be observed in the same table for frequency bands features. Altogether, these results demonstrate that EMD-based features, through their adapted bandwidth selection, fit better the individual characteristics. Indeed, IMFs convey a spectral information (notably the frequency bandwidth) that can significantly vary from one individual to the other. Then, as the ratios defined in expressions (3) solely imply IMFs indices, they can naturally adapt to the spectral specificities of each individual.

For better visual comparison, overall accuracies and κ values obtained with PSD and EMD-based feature sets are bar-plotted in Figures 4 and 5.

Another interesting outcome of this experiment is that in cross classification EMD-based energy ratios outperform the EMD-based energy bands whereas it is the opposite for self-classification. The overall accuracy and the κ values of EMD-based ratios are sensibly the same for self and cross classifications. With EMD-based energy bands, the performance decreases for the cross classification. This can be explained as follows. When test and training data are selected from different subjects, energies at some scales (mostly coarse scales corresponding to low frequency components) may substantially vary affecting thus the classification performance. With energy ratios however, since they combine the energies at different scales, this local energy variability is less penalizing.

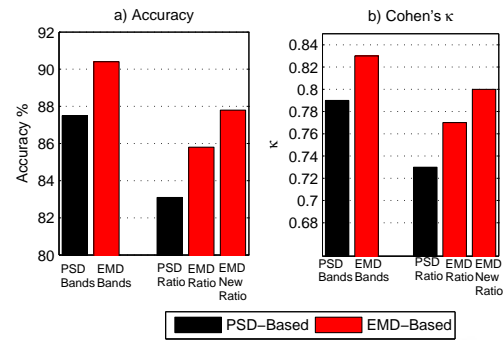


Figure 4: Final comparison of the classification performances (First group classification).

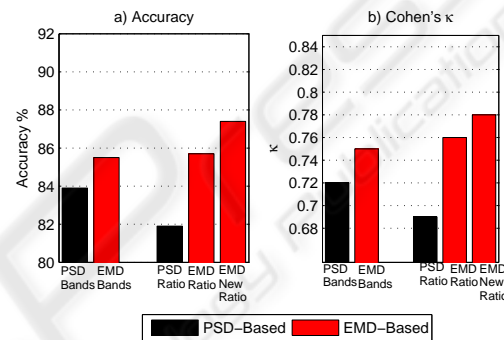


Figure 5: Final comparison of the classification performances (Second group classification).

5 CONCLUSIONS AND FUTURE WORKS

In this paper EMD is applied to rat EEG signals in order to extract features for sleep state classification. The results obtained from EMD-based features are compared to those obtained from PSD-based features, and show that EMD-based techniques are particularly adapted to analyze non-stationary signals, such as EEGs or any other biophysical signals. Since EMD is a data-driven technique that naturally decomposes the data into intrinsic components, it removes the necessity of a hazardous fixed band division. Adaptivity of EMD also yields a more robust classification with respect to the inter-individual variability.

In addition, as the sifting process performs locally in time, an on-line version of the EMD algorithm was proposed in (Rilling et al., 2003). Then, we could use this to adapt our EMD-based classifier to continuous time, with no prior segmentation of the signal needed. This approach would permit sleep state monitoring with real-time classification and detection of transition points.

Table 3: Self classification performances after using PSD-based spectral band energy features.

	AW	SWS	PS	ϵ_o	ϵ_c
AW	0.84±0.01	0.02±0.00	0.14±0.01	0.16±0.01	0.07±0.00
SWS	0.02±0.00	0.98±0.00	0.00±0.00	0.02±0.01	0.04±0.01
PS	0.20±0.01	0.01±0.00	0.79±0.01	0.21±0.02	0.42±0.01

Spc.=82.5%±0.4 Sns.=86.8%±0.4 Acc.=87.5%±0.4 κ =0.79±0.01

Table 4: Self classification performances after using EMD-based spectral band energy features.

	AW	SWS	PS	ϵ_o	ϵ_c
AW	0.91±0.01	0.03±0.00	0.06±0.01	0.09±0.01	0.08±0.01
SWS	0.04±0.01	0.96±0.01	0.00±0.00	0.04±0.01	0.06±0.01
PS	0.22±0.02	0.01±0.01	0.77±0.02	0.23±0.02	0.25±0.02

Spc.= 87.1%±0.7 Sns.=87.9%±0.7 Acc.=90.4%±0.4 κ =0.83±0.01

Table 5: Self classification performances after using PSD-based spectral energy ratios.

	AW	SWS	PS	ϵ_o	ϵ_c
AW	0.76±0.02	0.01±0.00	0.23±0.02	0.24±0.02	0.07±0.01
SWS	0.03±0.01	0.97±0.01	0.01±0.00	0.03±0.01	0.03±0.00
PS	0.16±0.02	0.00±0.01	0.84±0.02	0.16±0.03	0.53±0.02

Spc.=79.4%±0.6 Sns.=85.4%±0.8 Acc.=83.2%±0.9 κ =0.73±0.01

Table 6: Self classification performances after using EMD-based spectral energy ratios.

	AW	SWS	PS	ϵ_o	ϵ_c
AW	0.80±0.01	0.02±0.00	0.18±0.01	0.20±0.01	0.06±0.01
SWS	0.03±0.01	0.96±0.00	0.01±0.00	0.04±0.00	0.04±0.01
PS	0.12±0.02	0.01±0.00	0.88±0.02	0.12±0.02	0.46±0.02

Spc.=81.6%±0.9 Sns.=87.8%±1.0 Acc.=85.8%±0.9 κ =0.77±0.01

Table 7: Self classification performances after using EMD-based new ratios.

	AW	SWS	PS	ϵ_o	ϵ_c
AW	0.83±0.01	0.02±0.00	0.15±0.01	0.17±0.01	0.05±0.01
SWS	0.03±0.01	0.96±0.01	0.01±0.00	0.04±0.01	0.04±0.01
PS	0.11±0.02	0.01±0.00	0.89±0.02	0.11±0.02	0.41±0.02

Spc.=83.4%±0.7 Sns.=89.2%±0.9 Acc.=87.8%±0.6 κ =0.80±0.01

Table 8: Cross classification results. The data from five rats are used for training and the remaining rat's data is used for testing. The procedure repeated for all rats and the mean values are provided.

Methods	AW		SWS		PS		Mean	Mean	Acc.	κ
	Spc.	Sns.	Spc.	Sns.	Spc.	Sns.	Spc.	Sns.		
PSD-Bands	89.7	79.2	92.7	96	56.7	74.8	79.7	83.3	84.0	0.72
EMD-Bands	91.5	80.2	87.1	98.4	69.5	78.7	82.7	85.8	85.5	0.75
PSD-Ratios	89.5	73.6	98.2	91.4	47.5	81.8	78.4	82.3	81.9	0.69
EMD-Ratios	93.0	79.5	96.7	95.7	54.7	87.1	81.5	87.4	85.7	0.76
EMD-New	93.4	82.2	96.6	95.3	60.0	88.1	83.3	88.6	87.4	0.78

ACKNOWLEDGEMENTS

Süleyman Baykut's work is supported by "The Scientific and Technological Research Council of Turkey-The Department of Science Fellowships and Grant Programmes (TUBITAK-BIDEB)" with the programme # 2214.

REFERENCES

- Cohen, J. (1960). A coefficient of agreement for nominal scales. In *Educational and Psychological Measurement*. Vol. 20, pp. 37-46.
- Corsi-Cabrera, M., Pérez-Garci, E., Rio-Portilla, Y. D., Ugalde, E., and Guevara, M. A. (2001). EEG bands during wakefulness, slow-wave, and paradoxical sleep as a result of principal component analysis in the rat. In *Sleep*. Vol. 24, No. 4.
- Estrada, E., Nazeran, H., Nava, P., Behbehani, K., Burk, J., and Lucas, E. (2004). EEG feature extraction for classification of sleep stages. In *Proc. of the 26th Annual International Conference of the IEEE EMBS*. San Francisco, USA.
- Flandrin, P., Rilling, G., and Goncalves, P. (2003). Empirical mode decomposition as a filter bank. In *IEEE Sig. Proc. Lett.* Vol. 11, No. 2, Part 1, pp. 112- 114.
- Gervasoni, D., Lin, S., Ribeiro, S., Soares, E., Pantoja, J., and Nicolelis, M. (2004). Global forebrain dynamics predict rat behavioral states and their transitions. In *The Journal of Neuroscience*. Vol. 24, No. 49, pp. 11137-11147.
- Goeller, C. J. and Sinton, C. M. (1989). A microcomputer-based sleep stage analyser. In *Computer Methods and Programs in Biomedicine*. Vol. 29, No. 1, 316.
- Gottesmann, C., Lacoste, G., Rodrigues, L., Kirkham, P., Arnaud, C., and Rallo, J. L. (1976). Method of automatic analysis and quantification of wakefulness-sleep behavior in the rat. In *Rev. Electroencephalogr. Neurophysiol. Clin.* Vol. 6, pp. 37-49.
- Hese, P. V., Philips, W., Koninck, J. D., de Walle, R. V., and Lemahieu, I. (2001). Automatic detection of sleep stages using the EEG. In *Proc. of the 23rd Annual International Conference of the IEEE EMBS*. Istanbul, Turkey.
- Huang, N., Shen, Z., Long, S., Wu, M., Shih, H., Zheng, Q., Yen, N. C., Tung, C. C., and Liu, H. (1998). The empirical mode decomposition and hilbert spectrum for nonlinear and nonstationary time series analysis. In *Proc. Roy. Soc. London A*. Vol. 454, pp. 903-995.
- Neckelmann, D., Olsen, O. E., Fagerland, S., and Ursin, R. (1994). The reliability and functional validity of visual and semi-automatic sleep:wake scoring in the moll-wistar rat. In *Sleep*. Vol. 17, No. 2, pp. 12031.
- Ning, T., Joseph, D., and Bronzino, D. (1990). Bispectral analysis of the rat EEG during REM sleep. In *Proc. of the Annual International Conference of the IEEE EMBS*. Vol. 12, No. 5.
- Rilling, G., Flandrin, P., and Goncalves, P. (2003). On empirical mode decomposition and its algorithms. In *IEEE-EURASIP Workshop on Nonlinear Signal and Image Processing NSIP-03*. Grado.
- Robert, C., Guilpin, C., and Limoge, A. (1999). Automated sleep staging systems in rats. In *Journal of Neuroscience Methods*. Vol. 88, No.2, pp. 111-122.
- Ruigt, G. S. F., Proosdij, J. N. V., and Delft, A. M. L. V. (1989). A large scale, high resolution, automated system for rat sleep staging i. In *Methodology and technical aspects. Electroencephalogr. Clin. Neurophysiol.* Vol. 73, pp. 52-63.
- Sharabaty, H., Martin, J., Jammes, B., and Esteve, D. (2006). Alpha and theta wave localisation using hilbert-huang transform: Empirical study of the accuracy. In *Proc. of IEEE Information and Communication Technologies-ICTTA*. Vol. 1, pp. 1159-1164.
- Timo-Iaria, C., Negrao, N., Schmidek, W. R., Hoshino, K., de Menezes, C. E. L., and da Rocha, T. L. (1970). Phases and states of sleep in the rat. In *Physiol. Behav.* Vol. 5, pp. 1057-1062.
- Torres, A., Fiz, J. A., Jané, R., Galdiz, J. B., Gea, J., and Morera, J. (2007). Application of the empirical mode decomposition method to the analysis of respiratory mechanomyographic signals. In *Proc. of the 29th Annual International Conference of the IEEE EMBS*. Lyon, France.
- Vivaldi, E. A. and Bassi, A. (2006). Frequency domain analysis of sleep EEG for visualization and automated state detection. In *Proc. of the 28th Annual International Conference of the IEEE EMBS*. New York City, USA.
- Vyazovskiy, V. V., Borbély, A. A., and Tobler, I. (2002). Interhemispheric sleep EEG asymmetry in the rat is enhanced by sleep deprivation. In *J. Neurophysiology*. Vol. 88, pp. 2280-2286.
- Winson, J. (1974). Patterns of hippocampal theta rhythm in the freely moving rat. In *Electroencephalogr. Clin. Neurophysiol.* Vol. 36, pp. 291-301.
- Ziqiang, Z. and Puthusserypady, S. (2007). Analysis of schizophrenic EEG synchrony using empirical mode decomposition. In *Proc. of 15th Int. Conference on Digital Signal Processing*. pp. 131-134, Cardiff, England.